Thermodynamics of the inclusion of naphthoxazole derivatives in cucurbit[7]uril

Nataly Rubio and Antonio L. Zanocco*

Universidad de Chile, Facultad de Ciencias Químicas y Farmacéuticas, Departamento de Química Orgánica y Fisicoquímica, Casilla 233, Santiago - 1, Santiago, Chile

Termodinámica de la inclusión de los derivados naftoxazol en cucurbit[7]urilo

Termodinàmica de la inclusió dels derivats naftoxazol en cucurbit[7]uril

Recibido: 18 de junio de 2015; aceptado: 19 de junio de 2015

RESUMEN

La inclusión de dos derivados del naftoxazol en cucurbit[7] urilo se ha estudiado empleando métodos fluorescentes de estado estacionario. Estas moléculas presentan un comportamiento inusual de la emisión cuando se asocian al cucurbit[7]urilo, mostrando una disminución de la banda de fluorescencia correspondiente al estado localmente excitado, concomitante con la aparición de una nueva banda de fluorescencia desplazada al rojo, que aumenta cuando aumenta la concentración de cucurbit[7]urilo. Este resultado se interpreta en términos de un complejo de transferencia de carga intramolecular formado durante el tiempo de vida del huésped en el estado excitado, después de que el complejo de inclusión se ha producido. Las constantes de equilibrio para el complejo de inclusión se determinaron a partir del aumento de fluorescencia a diferentes temperaturas. Los parámetros termodinámicos obtenidos a partir de estos experimentos, indican que la inclusión de 2-metilnafto[1,2-d]oxazol, está determinada por factores entálpicos, mientras que fuerzas impulsoras clásicas de naturaleza entrópica, son dominantes en el proceso de inclusión de 2-fenilnafto[2,1-d]oxazol.

Palabras clave: Inclusión; derivados naftoxazol; cucurbitáceas[7]urilo

SUMMARY

The inclusion of two naphthoxazole derivatives in cucurbit[7]uril has been studied employing steady-state fluorescent methods. These guest present an unusual behavior of the emission, showing a decrease of the fluorescence band corresponding to the locally excited state, concomitant with the onset of a new red-shifted fluorescence band, that increases when the cucurbit[7]uril concentration increases. This result was interpreted in terms of an intramolecular charge-transfer complex formed during the lifetime of the excited dye, after the inclusion complex has been produced. The equilibrium constants for the inclusion complex were determined from the fluorescence increase at different temperatures. Thermodynamic parameters obtained from these experiments indicate that inclusion of 2-methylnaphtho[1,2-d]oxazole is determined by enthalpic factors whereas classical entropic driving forces are dominant in the inclusion process of 2-phenylnaphtho[2,1-d] oxazole.

Key words: Inclusion; naftoxazol derivatives; cucurbit[7] uril

RESUM

La inclusió de dos derivats del naftoxazol en cucurbit[7] uril s'ha estudiat emprant mètodes fluorescents d'estat estacionari. Aquestes molècules presenten un comportament inusual de l'emissió quan s'associen a cucurbit[7] uril mostrant una disminució de la banda de fluorescència corresponent a l'estat localment excitat, concomitant amb l'aparició d'una nova banda de fluorescència desplaçada al vermell, que augmenta quan augmenta la concentració de cucurbit[7]uril. Aquest resultat s'interpreta en termes d'un complex de transferència de càrrega intramolecular format durant el temps de vida de l'hoste en l'estat excitat, després que el complex d'inclusió s'ha produït. Les constants d'equilibri per al complex d'inclusió es van determinar a partir de l'augment de fluorescència a diferents temperatures. Els paràmetres termodinàmics obtinguts a partir d'aquests experiments, indiquen que la inclusió de 2-metilnafto[1,2-d] oxazol, està determinada per factors entàlpics, mentre que forces impulsores clàssiques de naturalesa entròpica, són dominants en el procés d'inclusió del 2-fenilnafto[2,1-d]oxazol.

Paraules clau: Inclusió; derivats naftoxazol; cucurbitàceas[7]uril

*Corresponding author: azanocco@ciq.uchile.cl; Phone: 56-2-29782878

INTRODUCTION

Since the publication of the molecular structure of cucurbit[6]uril by Mock in 1981, [1] cucurbit[n]urils, CBs, and their derivatives have attracted more and more attention. These macrocyclic container molecules composed of glycoluril monomers joined by pairs of methylene bridges, have a hydrophobic cavity accessible through two identical carbonyl-fringed portals, and form stable host–guest complex with a wide range of guest molecules [2-4]. Depending on the number of glycoluril units, homologues of different sizes are known, importantly CB5, CB6, CB7, and CB8. All CBs have a highly symmetrical, pumpkin-shaped structure, similar to cyclodextrins and calixarenes in their cone conformation [5]. In recent years, CBs have been established as versatile and interesting host molecules, which form stable inclusion complexes with small guest molecules such as organic dyes [6], metal cations [7-9], and protonated alkyl and arylamines [5, 10-11]. Several techniques have been employed to study the binding properties of cucurbituril in solution: NMR spectroscopy [12-14], calorimetry [15-17], and UV-vis absorption spectroscopy [18-20]. The effect of CBs on the photophysical and photochemical behavior on common neutral fluorescent dyes has been investigated to a lesser extension. Dye molecules immersed in the cavity of CBs experience an exceptionally low polarizability (near that of the gas phase) [21-23], which is expected to decrease the radiative decay rate constants. On the contrary, when CBs act as cation receptors, the interactions are stronger than those between protonated fluorescent dyes and cyclodextrins. For example, the results obtained from the ground-state absorption and steady-state as well as time-resolved fluorescence and anisotropy studies indicate that both the cationic and neutral form of neutral red, NRH^+ and NR, respectively, form strong inclusion complexes with CB7, particularly the protonated NRH^+ ($K > 10^5\ M^{-1}$) [24]. Cucurbit[7]uril enhances the fluorescence of several alkaloids such as palmatine and dehydrocorydaline, [25] berberine [17,26] and coptisine [27]. Furthermore, the presence of cucurbit[7]uril modifies the fluorescent properties of several classes of dyes such as styryls [28], alkyl meso-thiacarbocyanines [29], coumarine derivatives [4,30,31], rhodamine [32], and aromatic polycyclic compounds [33], among others. Benzo- and naphthoxazole derivatives are heterocyclic dyes with highly favorable photophysical properties, high fluorescence quantum yields and photostability and their photophysical properties can be easily tuned by changing the substituent at position 2 of the oxazole ring. Consequently, aryloxazole derivatives have been used as organic plastic scintillators [34] and optical fiber sensors [35,36]. Moreover, some of the derivatives are biologically active, showing activity as cytotoxic [37,38], antimicrobial [39,40], inhibitor on both eukaryotic DNA topoisomerase I and II [41] and genotoxic [42]. They have also been used as fluorescent probes of micelles, [43] thiols [44-47] and metal cations [48,49] and as fluorescence markers in biological systems [50,51]. However, their poor solubility in water requires the use of organic solvents (the simplest approach) is not compatible with biologically- or environmentally-relevant applications, and their use on large scales is frequently discouraged by economic and environmental considerations. The search for fluorescent molecules with high photostability and brightness in water, an environmentally-benign and biologically-relevant solvent is a topic of high interest. In this context, strategies involving stabilizing, solubilizing, disaggregating and enhancing additives have become very popular. We have studied the formation of supramolecular systems between naphthoxazole derivatives and CB7. The aims of this study are to account for the effect of the cucurbit[7]uril on the photophysical behavior of naphthoxazole derivatives, to determine the stoichiometry and binding constants of the inclusion complex, to determine the thermodynamic parameters associated to the inclusion process, and ultimately to study the effect of naphthoxazole structure (Figure 1) on the inclusion process.

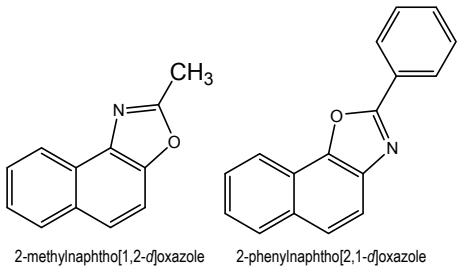

Figure1. *Molecular structures of naphthoxazole derivatives.*

EXPERIMENTAL

Reagents

All experiments were performed with analytical or spectroscopic grade chemicals. Cucurbit[7]uril was synthesized as described earlier [52], and its structure was probed by mass spectrometry. The synthetic procedure of the fluorescent probes 2-methylnaphtho[1,2-d]oxazole (MNOX) and 2-phenylnaphtho[1,2-d]oxazole (PHNOX) was previously described and were available in our laboratory. The purity of these dyes was checked by HPLC chromatography before use. Distilled water was purified trough a MilliQ system. Citrate buffer solutions (pH = 3) were prepared according to the current procedures. All other solvents used were of commercially available spectroscopic grade.

Apparatus

Absorption spectra were recorded in a Unicam UV 4 spectrophotometer using 1 cm quartz cells. Data were processed with Vision software. Steady-state fluorescence measurements were performed with a PC1 photon counting spectrofluorimeter from ISS, equipped with a thermostatic rectangular cell holder. The experiments were carried out in the range 20–40 °C, using a bath/circulation thermostat Haake K. The fluorescence spectra of each set of solutions were measured under identical experimental conditions. The excitation wavelength was set at the absorption spectrum maximum. Fluorescence decays were recorded with a time-correlated single photon counting system (Fluotime 200, PicoQuant GmbH, Berlin, Germany). Excitation was achieved by means of a 330 nm picosecond diode laser working at 10 MHz repetition rate. The counting frequency was kept always below 1%. Fluorescence lifetimes were analyzed using the PicoQuant FluoFit 4.0 software.

Solution preparation

The dye stock solutions were prepared by dissolving an appropriate amount of the oxazole derivative in metha-

nol. The stock solutions of CB7 in buffer were prepared with concentrations in the range 9 - 12 mM.

Inclusion complex preparation

Typically a set of 8 – 10 CB7 solutions was prepared in the range 0.15 – 4.5 mM with a constant dye concentration. The final solution was obtained in the following manner: 8 μL of a stock solution of the 1.5 mM naphthoxazole derivative in methanol were introduced into a 15 ml PTFE test tube and the solvent was then removed with a nitrogen stream. 100 – 1500 μL of the CB7 stock solution were then added to the dry dye, the solutions were homogenized in an ultrasonic bath at room temperature for 2 min and finally shaked at controlled temperature in a Hangzhou model MSC-100 thermoshaker for 24 hrs at 650 rpm.

RESULTS AND DISCUSION

Addition of CB7 to aqueous solutions of MNOX and PHNOX, did not produce any significant changes in their absorption spectra, although a slight increase in the absorbance with no spectral shift were observed. Under the same experimental conditions, the fluorescence spectra changed dramatically. As shown in Figure 2 for MNOX, the fluorescence band corresponding to the locally excited S1 state with λMax = 334 nm in buffer pH = 3, decreased with the concomitant appearance of a new wide band with maximum at 394 nm. The decrease of the band at 334 nm and the increase of the band at 394 nm depended on the CB7 concentration. This behavior was also found for PHNOX. Although for this naphthoxazole derivative the fluorescence quantum yield is lower than for MNOX in the absence of CB7, the decrease of the band corresponding to the locally excited state and the occurrence of a new broad band that increases substantially with the incremental addition of CB7 are evident (Figure 2).

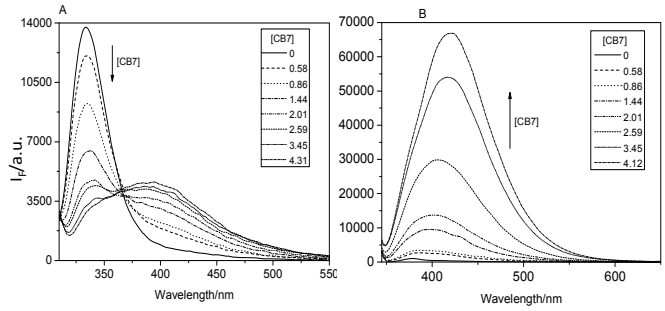

Figure 2. *Dependence of the fluorescence spectra of naphthoxazole derivatives on the CB7 concentration. A: MNOX, B: PHNOX.*

An almost 60-fold increase in the fluorescence intensity was observed for PHNOX. With only a few exceptions inclusion of dyes in the CB7 cavity leads to hypsocromic shifts in the fluorescence spectra, characteristic for the inclusion in a less polar environment, while the fluorescence quantum yields increase. The onset of a new wide fluorescence band and its increase in a CB7 concentration fashion reveal an interaction between CB7 and the dyes indicating the formation of an inclusion complex. The unexpected red-shifted new band can be understood in terms of the formation of a partial charge-transfer excited state. As was previously reported [43], the fluorescence spectra of naphthoxazole derivatives shows an important solvatochromic effect leading to large Stokes shifts and a large increase of the excited-state dipole moment in polar solvents, with the charge migrating from the naphthalene moiety to the oxazole ring, which it is compatible with the formation of an intramolecular charge-transfer excited state. An excited state of identical nature could be formed in the host-guest complex (see the schematic representation in Figure 3), possibly stabilized by interactions of the slightly polarizable inner CB7 cavity with the electron deficient naphthalene moiety and the electron rich oxazole ring with protons of the surrounding media at pH = 3

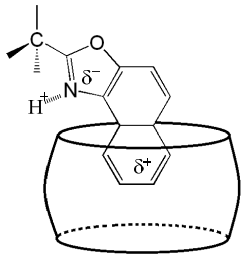

Figure 3. *Schematic representation of the inclusion complex formed between MNOX and CB7..*

In addition, interactions of the protonated oxazole with the carbonyl groups at the rim of the cucurbituril macrocycle could also contribute to the stabilization of intramolecular charge-transfer state during its lifetime. It is important to note that this process can occur only during the lifetime of the excited state, after the naphthoxazole derivative has been incorporated to the CB7 cavity. As shown in Figure 4, neither a bathochromic shift of the lower-energy absorption band of PHNOX nor the onset of new red-shifted bands are observed in the absorption spectra in the CB7 concentration range used. The λ_{Max} = 339 nm measured at CB7 concentration of 3.8 mM matches the λ_{Max} values measured in a large set of solvents.

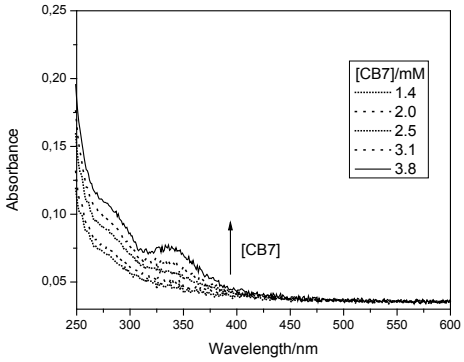

Figure 4*. Absorption spectra of PHNOX in the presence of CB7.*

Furthermore, we measured the fluorescence lifetime for MNOX in several solvents and buffer solutions with added CB7 (after equilibrium was obtained). We found monoexponential decays in pure solvents and buffer citrate pH = 3 with lifetimes equal to 6.8 ns (formamide), 6.1 ns (dioxane), 5.7 ns (methanol) and 5.2 ns (buffer citrate pH = 3). In the presence of CB7, we observed biexponential decays with τ_1 = 6.4 ns and τ_2 = 1.7 ns ([CB7] = 0.29 mM); τ_1 = 6.5 ns

and τ_2 = 1.6 ns ([CB7] = 1.4 mM); and τ_1 = 6.6 ns and τ_2 = 1.2 ns ([CB7] = 2.8 mM). Also, the ratio of signal intensities with CB7 present, I_2/I_1 increases from 3.6 ([CB7] = 0.29 mM) to 5.3 ([CB7] = 2.8 mM). These data show that: a) in the buffer solution only one transient is present, assigned to the S1 state of MNOX; b) with CB7 present, the shorter lifetime decreases when the CB7 concentration increases; and c) the relative amplitude of the component 2 increases with the CB7 concentration. We interpreted these results assigning the shorter-lifetime component to the intramolecular charge-transfer complex formed in the CB7 cavity.

Association constants determinations

The fluorescence increase can be described considering the inclusion complex formation between the naphthoxazole and CB7. Assuming an 1:1 association complex, the equilibrium can be described as:

$$NAPHTHOX + CB7 \overset{K_1}{\rightleftharpoons} [NAPHTHOX \cdots CB7] \qquad (1)$$

Equation (2) accounts for the fluorescence intensity change with CB7 concentration [53, 54].

$$I_f = \frac{I_f^o + I_1 * K_1[CB7]}{1 + K_1 * [CB7]} \qquad (2)$$

were I^0_f is the fluorescence intensity of the naphthoxazole derivative without CB7 added, I_1 is the expected fluorescence intensity from the 1:1 complex when all guest molecules form complexes with CB7, [CB7] is the concentration of CB7, and K_1 is the equilibrium constant for the inclusion complex formation. The equilibrium constant can be estimated using a nonlinear regression method to fit the fluorescence enhancement data. Figure 5 shows the integrated fluorescence area of MNOX as a function of CB7 concentration. The data are properly fitted with equation (2) from which K_1 was evaluated. The values of K_1 for MNOX are included in Table 1

Figure 6 shows the dependence of fluorescence enhancement of PHNOX on the CB7 concentration. As can be observed, the data do not fit equation (1) displaying an important upward deviation at high CB7 concentration. Deviation of experimental data from the equation for the formation of 1:1 complex suggests that a consecutive 1:2 complex formation may occur. In this instance, an additional equilibrium step should be considered:

$$[NAPHTHOX \cdots CB7] + CB7 \overset{K_{12}}{\rightleftharpoons} [CB7 \cdots NAPHTHOX \cdots CB7] \qquad (3)$$

If the formation of the 1:2 complex is considered, the fluorescence increase of PHNOX as function of CB7 concentration can be described in terms of equation (4):

$$I_f = \frac{I_f^0 + I_1 * K_1 * [CB7] + I_{12} * K_1 * K_{12} * [CB7]^2}{1 + K_1 * [CB7] + K_1 * K_{12} * [CB7]^2} \qquad (4)$$

were I^0_f, I_1, [CB7] and K_1 have been previously defined and I_{12} is the expected fluorescence intensity from the 1:2 complex when all guest molecules form complexes 1:2 with CB7 and K_{12} is the equilibrium constant for the 1:2 inclusion complex formation. Figure 4, in which the fluorescence increase does not reach the saturation plateau at the CB7 concentration employed, shows that the experimental data could be appropriately fitted by equation (4), from which both K_1 and K_{12} were obtained using a nonlinear regression method. The values of K_1 and K_{12} for PHNOX are collected in Table 1.

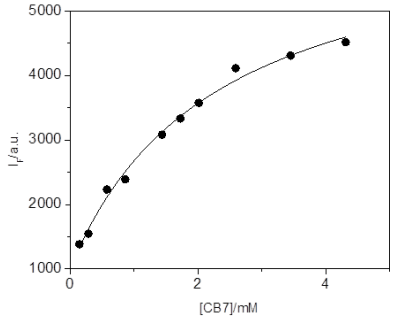

Figure 5. *Dependence of the integrated fluorescence spectra of MNOX on the CB7 concentration, [MNOX] = 21* **m***M. Solid line non-linear plot shows the best fit of the data to equation (2).*

The values of K_1 for MNOX and PHNOX are lower than that reported for the association of cationic dyes with CB7 [3] and in the order of the inclusion equilibrium constants previously measured for neutral molecules [22]. The results can be understood considering that the protonation at the oxazole ring can be safely ruled out in buffer citrate at pH = 3, as it is a weaker base (pKa = 0.8) [55], consequently, the neutral naphthoxazole derivative is included in the CB7 cavity.

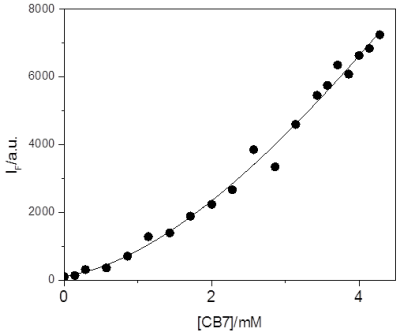

Figure 6. *Dependence of the integrated fluorescence spectra of PHNOX on the CB7 concentration, [PHNOX] = 13 mM. Solid line non-linear plot shows the best fit of the data to equation (4).*

Table 1.*Values of equilibrium constants for the inclusion of MNOX and PHNOX in CB7 at different temperatures.*

	MNOX	PHNOX	
T/K	K_1/M^{-1}	K_1/M^{-1}	K_{12}/M^{-2}
293	433 ± 39	114 ± 13	0.13 ± 0.02
298	421 ± 41	135 ± 18	0.16 ± 0.02
303	366 ± 51	189 ± 20	0.21 ± 0.03
413	308 ± 27	204 ± 17	0.23 ± 0.03

In addition we measured the equilibrium complex formation constant to gain insight into the factors controlling the thermodynamics of the reversible binding. The enthalpy changes of the studied 1:1 complexation reaction were obtained from van't Hoff plots (Figure 7).

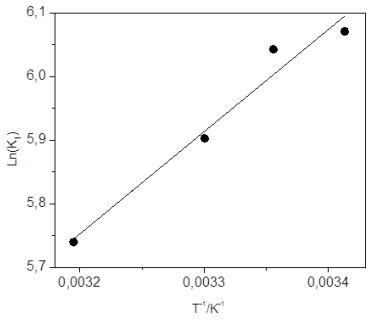

***Figure 7**. van't Hoff plot of the binding constants for MNOX-CB7 determined by fluorescence methods.*

The ΔH^0, ΔG^0 and $T\Delta S^0$ values are shown in Table 2. The values of the Gibbs free energy for the system at 298 K indicate a thermodinamically favorable reaction.

***Table 2.** Thermodynamic parameters for the formation of 1:1 inclusion complex between naphthoxazole derivatives and CB7.*

	MNOX	PHNOX
ΔG^0/KJ mol^{-1}	-14.9 ± 2	-12.2 ± 1.5
ΔH^0/KJ mol^{-1}	-13.7 ± 2	22.9 ± 3
T ΔS^0/KJ mol^{-1}	1.2 ± 0.2	-35.1 ± 4

The results indicate that enthalpic factors are the responsible for the inclusion of MNOX in CB7, whereas entropic factors are the dominant driving forces for the complex formation between PHNOX and CB7. The interaction between neutral guest and CBs has been barely explored. Recently, the nature of the driving forces for the complexation between CBs and neutral compounds has been discussed in depth [22-24, 56]. In these cases, the hydrophobic enthalpic factor has been mentioned as the main responsible driving force for complex formation. We interpreted our results considering that the dominant enthalpic factor, when MNOX is the guest, is a consequence of a greater amount of high-energy water molecules released from the CB7 cavity. MNOX can penetrate deeper than PHNOX in the host due to its smaller volume. With PHNOX as guest, the phenyl substituent and the larger volume restrict the complete guest inclusion, forming a partial inclusion or even a suspended complex. In these situations, classical hydrophobic effects are the main driving force. This picture of complex formation also explains the formation of 1:2 complexes at high CB7 concentration when PHNOX is the guest.

In conclusion, association of MNOX and PHNOX with CB7 is accompanied by an unusual behavior of the fluorescence spectra, compatible with the formation of an intramolecular charge-transfer complex inside the CB7 cavity, during the naphthoxazole derivative lifetime. The inclusion process is driven by enthalpic factors when MNOX is the guest and promoted by entropic classical hydrophobic effect when PHNOX is included, which can be related to the importance of the size of the substituent on the naphthoxazole ring in determining the nature of the process.

ACKNOWLEDGEMENTS

Financial support from FONDECYT (grant 1110636) is gratefully acknowledged.

BIBLIOGRAPHY

1. W.A. Freeman; W.L. Mock; N.Y. Shih; J. Am. Chem. Soc. 103, 7367-7368, 1981.
2. J. Kim; Y. Ahn; K.M. Park; Y. Kim; Y.H. Ko; D.H. Oh; K. Kim; Angew. Chem. Int. Ed. 46 7393-7395, 2007.
3. R.N. Dsouza; U. Pischel; W.M. Nau; Chem. Rev. 111, 7941–7980, 2011.
4. M.E. Aliaga; L. García-Río; M. Pessego; R. Montecinos; D. Fuentealba; I. Uribe; M. Martín-Pastor; O. García-Beltrán; New J. Chem. 39, 3084-3092, 2015.
5. J.W. Lee; S. Samal; N. Selvapalam; H.-J. Kim; K. Kim; Acc. Chem. Res. 36, 621-630, 2003.
6. V.F. Pais; E.F.A. Carvalho; J.P.C. Tomé; U. Pischel; Supramol. Chem. 26, 9, 642-647, 2014.
7. D. Whang; J. Heo; J.H. Park; K. Kim; Angew. Chem., Int. Ed. Engl. 37, 78-80, 1998.
8. Q. Li; Y.Q. Zhang; Q.J. Zhu; S.F. Xue; Z. Tao; X. Xiao; Chemistry-An Asian Journal, 10, 1159-1164, 2015.
9. K. Chen; Y.S. Kong; Y. Zhao; J.M. Yang; Y. Lu; W.Y. Sun; J. Am. Chem. Soc. 136, 16744-16747, 2014.
10. V. Lemaur; G. Carroy; F. Poussigue; F. Chirot; J. De Winter; L. Isaacs; P. Dugourd; J. Cornil; P. Gerbaux; ChemPlusChem 78, 959-969, 2013.
11. H.J. Buschmann; L. Mutihac; E. Schollmeyer; Thermochim. Acta 495, 28-32, 2009.
12. Q. Liu; Q. Tang; Y.Y. Xi; Y. Huang; X. Xiao; Z. Tao; S.F. Xue; Q.J. Zhu; J.X. Zhang; G. Wei; Supramol. Chem. 27, 386-392, 2015.
13. S. Riela; F. Arcudi; G. Lazzara; P. Lo Meo; S. Guernelli; F. D'Anna; S. Milioto; R. Noto; Supramol. Chem. 27, 233-243, 2015
14. D.D. Xiang; Q.X. Geng; H. Cong; Z. Tao; T. Yamato; Supramol. Chem. 27, 37-43, 2015.
15. L.C. Smith; D.G. Leach, B.E. Blaylock; E. Brittney; O.A. Ali; A.R. Urbach; J. Am. Chem. Soc. 137, 3663-3669, 2015.
16. N. Rawat; A. Kar; A. Bhattacharyya; A. Rao; S.K. Nayak; C. Nayak; S.N. Jha; D. Bhattacharyya; B.S. Tomar; Dalton Trans. 44, 4246-4258, 2015.
17. Z. Miskolczy; L. Biczók; Phys. Chem. Chem. Phys. 16, 20147-20156, 2014.
18. M. Gupta; D.K. Maity; S.K. Nayak; A.K. Ray; J. Photochem. Photobiol. A:Chem. 300, 15-21, 2015.
19. C. Gao; S. Silvi; X. Ma; H. Tian; A. Credi; M. Venturi; Chem.- Eur. J. 18, 16911-16921, 2012.
20. H. Liu; S.F. Xue; L. Mou; Z. Tao; Spectrosc. Spec. Anal. 30, 3351-3354, 2010.
21. K.I. Assaf; W.M. Nau; Supramol. Chem. 26, 657-669, 2014.
22. W.M. Nau; M. Florea; K.I. Assaf; Isr. J. Chem. 51, 559–577, 2011.
23. A.L. Koner; W.M. Nau; Supramol. Chem. 19, 55-66, 2007.
24. J. Mohanty; A.C. Bhasikuttan; W.M. Nau; H. Pal. J. Phys. Chem. B, 110, 5132-5138, 2006.
25. C.J. Li; J. Li; X.S. Jia; Org. Biomol. Chem. 7, 2699-2703, 2009.
26. Z. Miskolczy; L. Biczók; J. Phys. Chem. B 118, 2499–2505, 2014.
27. G.Q. Wang; Y.F. Qin; L.M. Du; J.F. Li; X. Jing; Y.X. Chang; H. Wu; Spectrochim. Acta A 98, 275-281, 2012.
28. A. Manna; S. Chakravorti; Spectrochim. Acta A 140, 241–247, 2015.

29. G.V. Zakharova; D.A. Zhizhimov; S.K. Sazonov; V.G. Avakyan; S.P. Gromov; H. Görner; A.K. Chibisov; J. Photochem. Photobiol. A: Chem. 302, 69–77, 2015.
30. A. Chatterjee; B. Maity; D. Seth; J. Phys. Chem. B, 118, 9768-9781, 2014.
31. N. Barooah; M. Sundararajan; J. Mohanty; A.C. Bhasikuttan; J. Phys. Chem. B 118, 7136-7146, 2014.
32. M. Gupta; K.K. Jagtap; V. Sudarsan; A. K Ray; Pramana J. Phys. 82, 277-281, 2014.
33. V.N. Sueldo Occello; R.H. de Rossi; A.V. Veglia; J. Lumin. 158, 435–440, 2015.
34. A. Pladalmau; J. Org. Chem. 60 5468-5473, 1995.
35. Y. Wang; K.M. Wang; W.H. Liu; G.L. Shen; R.Q. Yu; Analyst 122 69-75, 1997.
36. Y. Wang; W.H. Liu; K.M. Wang; G.L. Shen; R.Q. Yu; Fresenius J. Anal. Chem. 361, 827-827, 1998.
37. M.M. Muir; O. Cox; L.A. Rivera; M.E. Cadiz; E. Medina; Inorg. Chim. Acta 191, 131-139, 1992.
38. C.M. Lozano; O. Cox; M.M. Muir; J.D. Morales; J.L. Rodriguez-Caban; P.E. Vivas-Mejia; F.A. Gonzalez; Inorg. Chim. Acta 271, 137-144, 1998.
39. I. Oren; I. Yalcin; E. Sener; N. Altanlar; Eur. J. Pharm. Sci. 7 153–160, 1998.
40. E.A. Sener; O.T. Arpaci; I. Yalcin; N. Altanlar; Farmaco 55, 397-405, 2000.
41. E. Oksuzoglu; B. Tekiner-Gulbas; S. Alper; O. Temiz-Arpaci; T. Ertan; I. Yildiz; N. Diril; E. Sener-Aki; I. Yalcin J. Enzym. Inhib. Med. Chem. 23, 37-42, 2008.
42. E. Oksuzoglu; O. Temiz-Arpaci; B. Tekiner-Gulbas; H. Eroglu; G. Sen; S. Alper; I. Yildiz; N. Diril; E. Aki-Sener; I. Yalcin; Med. Chem. Res. 16 1-14, 2007.
43. M. Curitol; X. Ragas; S. Nonell; N. Pizarro; M. V. Encinas; P. Rojas; R. P. Zanocco; E. Lemp; G. Gunther; A. L. Zanocco; Photochem. Photobiol. 89, 1327–1334, 2013.
44. S.C. Liang; H. Wang; Z.M. Zhang; X. Zhang; H.S. Zhang; Anal. Chim. Acta 451, 211-219, 2002.
45. S.C. Liang; H. Wang; Z.M. Zhang; H.S. Zhang; Anal. Bioanal. Chem. 381, 1095-1100, 2005.
46. S.C. Liang; H. Wang; Z.M. Zhang; M. Zhang; H.S. Zhang Spectroc. Acta A 58 2605-2611, 2002.
47. M. Szabelski; M. Rogiewicz; W. Wiczk; Anal. Biochem. 342 20-27, 2005.
48. K. Tanaka; T. Kumagai; H. Aoki; M. Deguchi; S. Iwata; J. Org. Chem. 66, 7328-7333, 2001.
49. M. Milewska; A. Skwierawska; K. Guzow; D. Smigiel; W. Wiczk; Inorg. Chem. Commun. 8, 947-950, 2005.
50. K. Guzow; M. Szabelski; J. Malicka; J. Karolczak; W. Wiczk; Tetrahedron 58 2201-2209, 2002.
51. K. Guzow; D. Szmigiel; D. Wroblewski; M. Milewska; J. Karolczak; W. Wiczk; J. Photochem. Photobiol. A: Chem. 187, 87-96, 2007.
52. J. Kim; I.-S. Jung; S.-Y. Kim; E. Lee; J.-K. Kang; S. Sakamoto; K. Yamaguchi; K. Kim; J. Am. Chem. Soc. 122, 540–541, 2000.
53. A. V. Deshpande; L. V. Jathar; J. R. Rane; J. Fluoresc. 2009, 19, 607-614.
54. A. Muñoz de la Peña; F. Salinas; M.J. Gómez; M.I. Acedo; M. Sánchez Peña; J. Incl. Phenom. Mol. Rec. Chem. 15, 131-143, 1993.
55. P.M. Dewick in Essentials of Organic Chemistry; John Wiley & Sons; West Susex; England p. 433, 2006.
56. F. Biedermann; V.D. Uzunova; O.A. Scherman; W.M. Nau; A. De Simone; J. Am. Chem. Soc. 134, 15318–15323, 2012.